Strange quark contributions to nucleon mass and spin from lattice QCD

M. Engelhardt

Phys. Rev. D **86**, 114510 — Published 20 December 2012

DOI: 10.1103/PhysRevD.86.114510

Strange quark contributions to nucleon mass and spin from lattice QCD

M. Engelhardt

Department of Physics, New Mexico State University, Las Cruces, NM 88003, USA

October 31, 2012

Abstract

Contributions of strange quarks to the mass and spin of the nucleon, characterized by the observables f_{T_s} and Δs, respectively, are investigated within lattice QCD. The calculation employs a 2+1-flavor mixed-action lattice scheme, thus treating the strange quark degrees of freedom in dynamical fashion. Numerical results are obtained at three pion masses, $m_\pi = 495\,\mathrm{MeV}$, $356\,\mathrm{MeV}$, and $293\,\mathrm{MeV}$, renormalized, and chirally extrapolated to the physical pion mass. The value extracted for Δs at the physical pion mass in the $\overline{MS}$ scheme at a scale of $2\,\mathrm{GeV}$ is $\Delta s = -0.031(17)$, whereas the strange quark contribution to the nucleon mass amounts to $f_{T_s} = 0.046(11)$. In the employed mixed-action scheme, the nucleon valence quarks as well as the strange quarks entering the nucleon matrix elements which determine f_{T_s} and Δs are realized as domain wall fermions, propagators of which are evaluated in MILC 2+1-flavor dynamical asqtad quark ensembles. The use of domain wall fermions leads to mild renormalization behavior which proves especially advantageous in the extraction of f_{T_s}.

PACS: 12.38.Gc, 14.20.Dh

1 Introduction

Strange quarks represent the lightest quark flavor not present in the valence component of the nucleon. Their study can thus provide insight into sea quark effects in the nucleon in isolated fashion. The two most fundamental properties of the nucleon are its mass and spin. The investigation presented here focuses on the extent to which those two properties are influenced by the strange quark degrees of freedom. The strange contributions to nucleon mass and spin can be characterized by the matrix elements

$$f_{T_s} = \frac{m_s}{m_N} \left[\langle N | \int d^3y \, \bar{s}s | N \rangle - \langle 0 | \int d^3y \, \bar{s}s | 0 \rangle \right] \tag{1}$$

and

$$\Delta s = \langle N, j | \int d^3y \, \bar{s}\gamma_j\gamma_5 s | N, j \rangle \tag{2}$$

respectively, where $|N, j\rangle$ denotes a nucleon state with spin polarized in the j-direction. In the case of the scalar matrix element, the vacuum expectation value, i.e., the vacuum strange scalar condensate, is subtracted; the intention is, of course, to measure the strangeness content of the nucleon *relative* to the vacuum. In the case of the axial matrix element, no subtraction is necessary since the corresponding vacuum expectation value vanishes. Note that Δs measures specifically the contribution of strange quark spin to nucleon spin; strange quark angular momentum constitutes a separate contribution not considered here.

Aside from representing a fundamental characteristic of the nucleon in its own right, the scalar strange content f_{T_s} is also an important parameter in the context of dark matter searches [1–4]. Assuming that the coupling of dark matter to baryonic matter is mediated by the Higgs field, the dark matter detection rate depends sensitively on the quark scalar matrix elements in the nucleon, cf., e.g, the neutralino-nucleon scalar cross-section considered in [1]. One a priori reasonable scenario is that the strange quark furnishes a particularly favorable channel [1], since, on the one hand, it features a much larger Yukawa coupling to the Higgs field than the light quarks, and, on the other hand, is not so heavy as to be only negligibly represented in the nucleon's sea quark content. As a consequence, an accurate estimate of f_{T_s} is instrumental in assessing the discovery potential for dark matter candidates.

The contribution of strange quark spin to nucleon spin Δs is, in principle, more directly accessible to experiment than f_{T_s}. Δs represents the first moment of the strange quark helicity distribution $\Delta s(x)$ (including both quarks and antiquarks) as a function of the momentum fraction x. The helicity distribution can be determined via inclusive deep inelastic scattering and semi-inclusive deep inelastic scattering [5–7]. However, its extraction in practice still has to rely to a certain extent on assumptions about the dependence of $\Delta s(x)$ on x, even in the semi-inclusive channels (which furnish direct information on $\Delta s(x)$), because of the limitations in accessing small x experimentally. Complementary information about Δs is obtained from the strange axial form factor of

the nucleon $G_A^s(Q^2)$, which can be extracted by combining data from parity-violating elastic electron-proton scattering and elastic neutrino-proton scattering [8]. Extrapolation to zero momentum transfer, $Q^2 = 0$, again yields an estimate of Δs. Depending on the specific extrapolations and/or model assumptions adopted in determining Δs via the various aforementioned avenues, both significantly negative values for Δs have been put forward [5, 9], as well as values compatible with zero [6]. An independent determination of Δs via lattice QCD, as undertaken in the present work, thus can be useful in several ways. Apart from shedding light on the fundamental question of the decomposition of nucleon spin, it can contribute constraints to phenomenological fits of polarized parton distribution functions. Furthermore, it influences spin-dependent dark matter cross sections [3]; although more accurate determinations of the scalar matrix elements discussed further above constitute the most urgent issue in reducing hadronic uncertainties in dark matter searches, Δs also plays a significant role in that context.

A number of lattice QCD investigations of strange quark degrees of freedom in the nucleon have recently been undertaken [10–26], the majority of which have focused specifically on the scalar content. Studies of the latter have proceeded via two avenues: On the one hand, one can directly determine the matrix element $\langle N|\bar{s}s|N\rangle$ via the appropriate disconnected three-point function; this methodology was adopted in[1] [10, 12,14–17,19,22,24] and also in the present work, as described in detail further below. A study of techniques suited to improve the efficiency of this approach has been presented in [27]. On the other hand, a somewhat less direct inference of the scalar strange quark content of the nucleon is possible via the study of the baryon spectrum, which is related via the Feynman-Hellmann theorem

$$\langle B|\bar{q}q|B\rangle = \frac{\partial m_B}{\partial m_q} \tag{3}$$

to the corresponding sigma terms for the baryon state $|B\rangle$ and quark flavor q. This avenue has been pursued in [13,15,21,23], and a related methodology, combining lattice hadron spectrum data with chiral perturbation theory, was pursued in [25, 26].

The characteristics of these various investigations of the scalar strange quark content of the nucleon are diverse. They include $N_f = 2$ calculations, in which the strange quark degrees of freedom are quenched [12–14,24], but also $N_f = 2{+}1$ [10,15–17,19,21,23,25,26] and even $N_f = 2{+}1{+}1$ [17,22] calculations. In some cases, lattice data at only one pion mass have been obtained to date and no extrapolation to the physical point has been attempted. The most stringent results obtained at the physical point including fully dynamical strange quarks were reported in [15, 17, 26]. Ref. [17] quotes $m_N f_{T_s}/m_s = 0.637(55)(74)$ in the $N_f = 2+1$ case, and $m_N f_{T_s}/m_s = 0.44(8)(5)$ in the $N_f = 2+1+1$ case; translated to f_{T_s} itself using $m_s = 95\,\mathrm{MeV}$ in the $\overline{MS}$ scheme at a scale of $2\,\mathrm{GeV}$ [28], these correspond to $f_{T_s} = 0.064(6)(7)$ for $N_f = 2+1$ and $f_{T_s} = 0.044(8)(5)$ for $N_f = 2{+}1{+}1$. On the other hand, [15] and [26] report significantly lower values. In [15],

[1] Strictly speaking, the method adopted in [16,17] constitutes a hybrid of the two methods.

both direct three-point function calculations as well as indirect determinations via the Feynman-Hellmann theorem are used to arrive at a bound $f_{T_s} = 0.009(15)(16)$. In [26], a more indirect analysis using lattice hadron spectrum data and chiral perturbation theory yields $m_N f_{T_s} = 21(6)\,\mathrm{MeV}$, which translates to $f_{T_s} = 0.022(6)$. The results obtained in the present work are of comparable accuracy, $f_{T_s} = 0.046(11)$, cf. (37), and are more consistent with the higher values reported in [17].

The strange axial matrix element Δs, on the other hand, has also been investigated in [10,11,24]. Apart from the exploratory study [10], which, however, did not attempt to renormalize the results nor extrapolate them to the physical pion mass, these investigations were based on dynamical quark ensembles containing only the two light flavors in the quark sea; the present lattice investigation, on the other hand, employs $N_f = 2 + 1$ gauge ensembles, thus treating the strange quark degrees of freedom in dynamical fashion. The numerical results for Δs obtained on this basis are renormalized and chirally extrapolated, yielding the estimate $\Delta s = -0.031(17)$, cf. (38), at the physical point in the $\overline{MS}$ scheme at a scale of 2 GeV. Within the uncertainties, this nevertheless remains compatible with the values obtained in the aforementioned other studies, though it is about 50% larger in magnitude. This suggests that systematic adjustments to the results quoted in those works through unquenching of the strange quark degrees of freedom, renormalization, and chiral extrapolation are not severe.

Aside from the two quantities f_{T_s} and Δs considered in the present work, lattice investigations of the strange quark structure within the nucleon have also considered generalizations to non-zero momentum transfer, i.e., form factors [18, 24], including calculations of the strange electric and magnetic form factors, which are of interest in the context of corresponding experimental efforts employing parity-violating electron-proton scattering [29]. Furthermore, also the strange quark momentum fraction and strange quark angular momenta in the nucleon have been investigated [20].

The present lattice investigation, a preliminary account of which was given in [30], is based on a mixed-action scheme developed and employed extensively by the LHP Collaboration [31–33]. The nucleon valence quarks as well as the strange quark fields appearing in the operator insertions in eqs. (1) and (2) are realized as domain wall fermions, propagators of which are evaluated in the background of (HYP-smeared) 2+1-flavor dynamical asqtad quark ensembles provided by the MILC Collaboration. Though computationally expensive, domain wall fermions lead to benign renormalization properties which prove especially advantageous in the case of the f_{T_s} observable; the substantial systematic uncertainties due to strong additive quark mass renormalizations encountered in analogous calculations using Wilson fermions [12, 24] are avoided. The computational scheme is described in detail in section 2. Section 3 provides the raw numerical results, the renormalization of which is discussed in section 4. The renormalized results are extrapolated to the physical pion mass in section 5, and systematic uncertainties and adjustments are considered in section 6, with conclusions presented in section 7.

2 Computational scheme

2.1 Correlator ratios

The lattice calculation of the nucleon matrix elements in (1), (2) proceeds in standard fashion via correlator ratios of the type

$$R[\ \Gamma^{nuc}, \Gamma^{obs}\ ](\tau, T) = \frac{\left\langle\ \left[\Gamma^{nuc}_{\alpha\beta}\ \Sigma_{\vec{x}}\ N_\beta(\vec{x}, T)\bar{N}_\alpha(0,0)\right] \cdot \left[-\Gamma^{obs}_{\gamma\rho}\Sigma_{\vec{y}}\ s_\rho(\vec{y}, \tau)\bar{s}_\gamma(\vec{y}, \tau)\right]\ \right\rangle}{\left\langle\ \Gamma^{unpol}_{\alpha\beta}\ \Sigma_{\vec{x}}\ N_\beta(\vec{x}, T)\bar{N}_\alpha(0,0)\ \right\rangle} \quad (4)$$

with nucleon interpolating fields N of the standard form (quoting here, for definiteness in flavor structure, the proton case)

$$N_\gamma = \epsilon_{abc} u^c_\gamma u^a_\alpha \left(C\gamma_5\right)_{\alpha\beta} d^b_\beta \quad (5)$$

where C denotes the charge conjugation matrix. The sums over spatial position $\vec{x}$ project the nucleon states onto zero momentum, whereas the sum over spatial position $\vec{y}$ is simply transcribed from (1), (2). Since the nucleon contains no strange valence quarks, the three-point function averaged in the numerator of (4) factorizes, as written, into the nucleon two-point function and the strange quark loop. I.e., only the disconnected diagram, cf. Fig. 1, contributes to the matrix elements under consideration. The strange

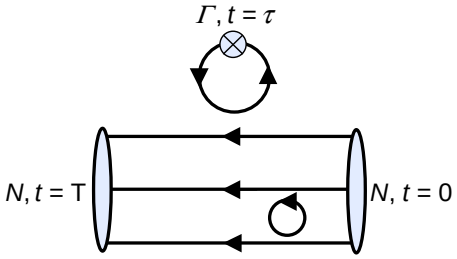

Figure 1: Disconnected contribution to nucleon matrix elements. The nucleon propagates between a source at $t = 0$ and a sink at $t = T$; the insertion of $\Gamma \equiv \Gamma^{obs}$ occurs at an intermediate time $t = \tau$.

quark fields have already been reordered in the numerator of (4) such as to make the standard minus sign associated with quark loops explicit. Finally, the Γ matrices allow one to choose the appropriate nucleon polarization and strange quark operator insertion structures. The denominator of (4) corresponds to the unpolarized nucleon two-point function, obtained using

$$\Gamma^{unpol} = \frac{1 + \gamma_4}{2}\ . \quad (6)$$

In the numerator, for the purpose of evaluating f_{T_s}, unpolarized nucleon states are appropriate, corresponding to the choice $\Gamma^{nuc} = \Gamma^{unpol}$; furthermore, the scalar strange quark insertion is obtained by choosing $\Gamma^{obs} = 1$,

$$\frac{m_s}{m_N} \left(R[\ \Gamma^{unpol}, 1\ ](\tau, T) \ - \ [\mathrm{VEV}] \right) \ \equiv \ R\{f_{T_s}\} \ \stackrel{T \gg \tau \gg 0}{\longrightarrow} \ f_{T_s} \tag{7}$$

with the vacuum expectation value

$$[\mathrm{VEV}] = \langle -\Sigma_{\vec{y}} \ s_\gamma(\vec{y}, \tau) \bar{s}_\gamma(\vec{y}, \tau) \rangle \tag{8}$$

to be subtracted.

On the other hand, Δs is obtained by using the projector onto nucleon states polarized in the positive/negative j-direction in the numerator of (4),

$$\Gamma^{nuc} = \frac{1 \mp i\gamma_j\gamma_5}{2} \Gamma^{unpol} \ , \tag{9}$$

as well as the operator insertion structure $\Gamma^{obs} = \gamma_j\gamma_5$. Averaging over positive/negative j-direction (with a relative minus sign) as well as the three spatial j to improve statistics leads one to evaluate

$$-i \ \cdot 2 \cdot \frac{1}{3} \sum_{j=1}^{3} R[\ (-i\gamma_j\gamma_5/2)\ \Gamma^{unpol}, \gamma_j\gamma_5\ ](\tau, T) \ \equiv \ R\{\Delta s\} \ \stackrel{T \gg \tau \gg 0}{\longrightarrow} \ \Delta s \ , \tag{10}$$

where the prefactor 2 compensates for the fact that the ratio (4) is normalized using the unpolarized nucleon two-point function in the denominator, even when the numerator is restricted to a particular polarization. Lastly, the prefactor $(-i)$ cancels the additional factor i which the γ_5-matrix in the operator insertion acquires when the calculation is cast in terms of Euclidean lattice correlators; thus, the Δs obtained through (10) is already Wick-rotated back to Minkowski space-time. Note that (10) does not call for the subtraction of a vacuum expectation value, since the latter vanishes in the ensemble average. In practice, this numerical zero was nevertheless subtracted from (10) in order to reduce statistical fluctuations.

2.2 Lattice setup

The averages in the correlator ratios (4) were carried out using the three MILC $2+1$-flavor dynamical asqtad quark ensembles listed in Table 1. HYP-smearing was applied to the configurations. Both the valence quarks in the nucleon two-point functions and the strange quark fields appearing in the matrix elements (1) and (2) were implemented using the domain wall fermion discretization, with parameters $L_5 = 16$, $M_5 = 1.7$. The domain wall quark masses, also listed in Table 1, are fixed by the requirement of reproducing the pion masses corresponding to the MILC ensembles [31]. This mixed action setup has

am_l^{asq}	am_s^{asq}	am_l^{DWF}	am_s^{DWF}	m_π	# configs	m_N
0.007	0.05	0.0081	0.081	293 MeV	468	1107 MeV
0.01	0.05	0.0138	0.081	356 MeV	448	1155 MeV
0.02	0.05	0.0313	0.081	495 MeV	486	1288 MeV

Table 1: $N_f = 2+1$, $20^3 \times 64$ MILC asqtad ensembles with lattice spacing $a = 0.124\,\mathrm{fm}$ used in the present investigation. Uncertainties in the pion and nucleon masses extracted from the corresponding two-point functions are under 1%.

been employed extensively for studies of hadron structure by LHPC [31,33] and further details concerning its tuning can be found in the mentioned references.

The space-time layout of the calculation is shown in Fig. 2. The strange quark loop trace was evaluated using stochastic estimation. Positioning the nucleon source at time $t = 0$, bulk complex $Z(2)$ stochastic sources with support in all of space within the temporal range $t = 3, \ldots, 7$ were introduced. This corresponds to averaging the correlator ratio (4) with respect to the operator insertion time τ over the aforementioned time slices (after having duly divided out the length of the temporal range). The stochastic estimate of the strange quark loop trace was performed employing 1200 of the described stochastic source vectors per gauge sample. In particular, obtaining a signal for Δs depends on accumulating high statistics in the stochastic estimator. The scalar matrix element, on the other hand, requires less statistics in the strange quark loop trace, but is more susceptible to gauge fluctuations. The sink time T at which the nucleon two-point functions are contracted and projected onto zero momentum remains variable in this layout.

While this scheme provides a high amount of averaging in relation to the number of strange quark propagator inversions, it precludes testing for a plateau in the three-point function by varying the operator insertion time τ. The positioning of the bulk stochastic source was motivated by previous work [31, 33] in the same mixed-action scheme, which investigated (connected contributions to) a wide variety of observables, and the results of which indicate that, having evolved in time from $t = 0$ to $t = 3$, excited state contaminations in the system are already small compared to the statistical uncertainty of the calculation performed here. To achieve this suppression of excited state contributions, the quark fields in the nucleon sources (5) are Wuppertal-smeared such as to optimize the overlap with the nucleon ground state [31–33]. Despite the relative positioning of the nucleon source and the strange quark insertion time range being fixed in this manner, it does nevertheless remain possible to exhibit the extent to which results depend on the separation between operator insertion and nucleon sink time T, which is still variable in the present scheme. Correlator ratios will be shown further below as a function of T, with asymptotic behavior being seen to emerge three lattice time steps beyond the end of the operator insertion range, i.e., for sink times

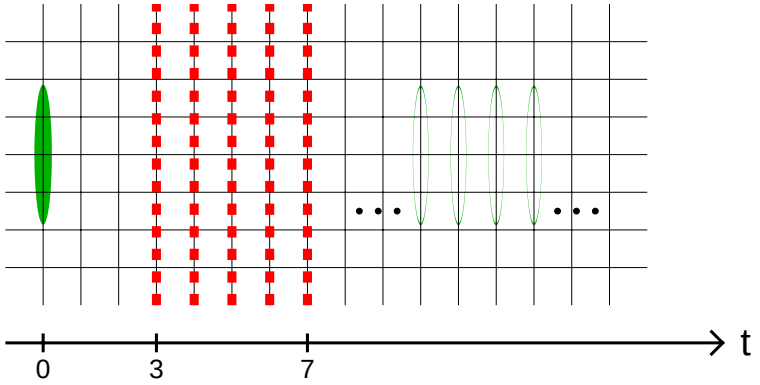

Figure 2: Setup of the lattice calculation. The nucleon source is located at lattice time $t = 0$. An average over operator insertion times τ is performed in the range $\tau = 3, \ldots, 7$; accordingly, stochastic sources are distributed over the bulk of the lattice in this entire time range. The temporal position T of the nucleon sink is variable.

$T \geq 10$. This corroborates the suitability of the choice for the bulk stochastic source time range adopted in the present calculation.

The correlator ratio (4) exhibits statistical fluctuations not only due to the strange quark loop factor discussed above, but also due to the nucleon two-point function factors. To reduce these fluctuations, it is equally necessary to sample the latter to a sufficient extent. To this end, multiple samples of the nucleon two-point function were obtained by employing eight different spatial positions for the nucleon source on the source time slice. In addition to this eight-fold sampling of the nucleon two-point function, the described scheme can be accomodated several times in temporally well-separated regions on the lattice; in practice, three replicas of the entire setup specified above were placed on the lattice, separated by 16 lattice spacings in the time direction, thus further enhancing statistics. Each gauge configuration therefore yielded altogether 24 samples of the numerator and denominator in the correlator ratio (4). Note again that averaging was further improved in the case of Δs by taking into account nucleon polarization axes aligned with all three coordinate axes, as already made explicit in (10).

3 Numerical results

The numerical results for the correlator ratios $R\{f_{T_s}\}$ and $R\{\Delta s\}$, cf. (7) and (10), averaged over the insertion time τ as described in section 2.2, are shown in Figs. 3 and 4 as a function of sink time T. The correlator ratios start out near vanishing values at small sink times T, and then accumulate strength as T traverses the region of support of the stochastic strange quark source. Beyond this region, $R\{f_{T_s}\}$ and $R\{\Delta s\}$ begin to level off and approach their asymptotic values f_{T_s} and Δs, respectively. There is only

a limited time window in which the latter behavior can be observed due to the increase in statistical fluctuations for large T.

m_π	$R\{\Delta s\}\|_{T=10}$	$R\{\Delta s\}\|_{T=10,\ldots,12}$
293 MeV	-0.023(17)	-0.023(25)
356 MeV	-0.030(9)	-0.030(12)
495 MeV	-0.021(4)	-0.022(5)

Table 2: Correlator ratio $R\{\Delta s\}$ at sink time $T = 10$, and averaged over $T = 10, \ldots, 12$. In the latter case, the error estimate is obtained by the jackknife method, i.e., the correlations between values of $R\{\Delta s\}$ at neighboring sink times are taken into account.

The correlator ratio $R\{\Delta s\}$ consistently behaves in line with the expectation advanced in section 2.2, namely, there is no significant trend in the correlator ratio beyond $T = 10$. This is quantified in Table 2, which compares the value of $R\{\Delta s\}$ at $T = 10$ with its $T = 10, \ldots, 12$ average.

The behavior of the lattice data for the correlator ratio $R\{f_{T_s}\}$ is not as smooth as in the case of $R\{\Delta s\}$. In particular, in the $m_\pi = 356\,\mathrm{MeV}$ correlator ratio, one notices an enhancement in the $T = 12, \ldots, 14$ region compared with the value at $T = 10$. On the other hand, both in the $m_\pi = 495\,\mathrm{MeV}$ and the $m_\pi = 293\,\mathrm{MeV}$ data, plateaux appear to be reached at $T = 10$. Table 3 again provides a comparison of the $T = 10$ value of $R\{f_{T_s}\}$ with its $T = 10, \ldots, 12$ average; in the case of $m_\pi = 356\,\mathrm{MeV}$, the results are barely compatible within the statistical uncertainties. Nevertheless, an interpretation of this behavior as a statistical fluctuation, as opposed to a systematic effect, seems most plausible: The direction of the deviations from the expected plateau behavior in the correlator ratio beyond $T = 10$ is not consistent across the data sets, with $R\{f_{T_s}\}$ decreasing slightly for $m_\pi = 495\,\mathrm{MeV}$, while it rises in the other two cases. Furthermore, there is no clear trend as a function of pion mass, with the largest upward deviation occuring for the middle pion mass, $m_\pi = 356\,\mathrm{MeV}$, while at $m_\pi = 293\,\mathrm{MeV}$ the deviation is again quite small.

In summary, thus, at the level of statistical uncertainty achieved in the present calculation, no systematic excited state effects stemming from a too restricted source-sink separation can be reliably extracted; or, in other words, such effects are smaller than the aforementioned statistical uncertainties. In view of this, in the following, the $T = 10$ values of the correlator ratios $R\{\Delta s\}$ and $R\{f_{T_s}\}$, as reported in Tables 2 and 3, will be regarded as the most reliable estimates for their asymptotic limits Δs and f_{T_s}, respectively. Systematic uncertainties, including the ones due to excited states, will be revisited and discussed in detail in section 6.

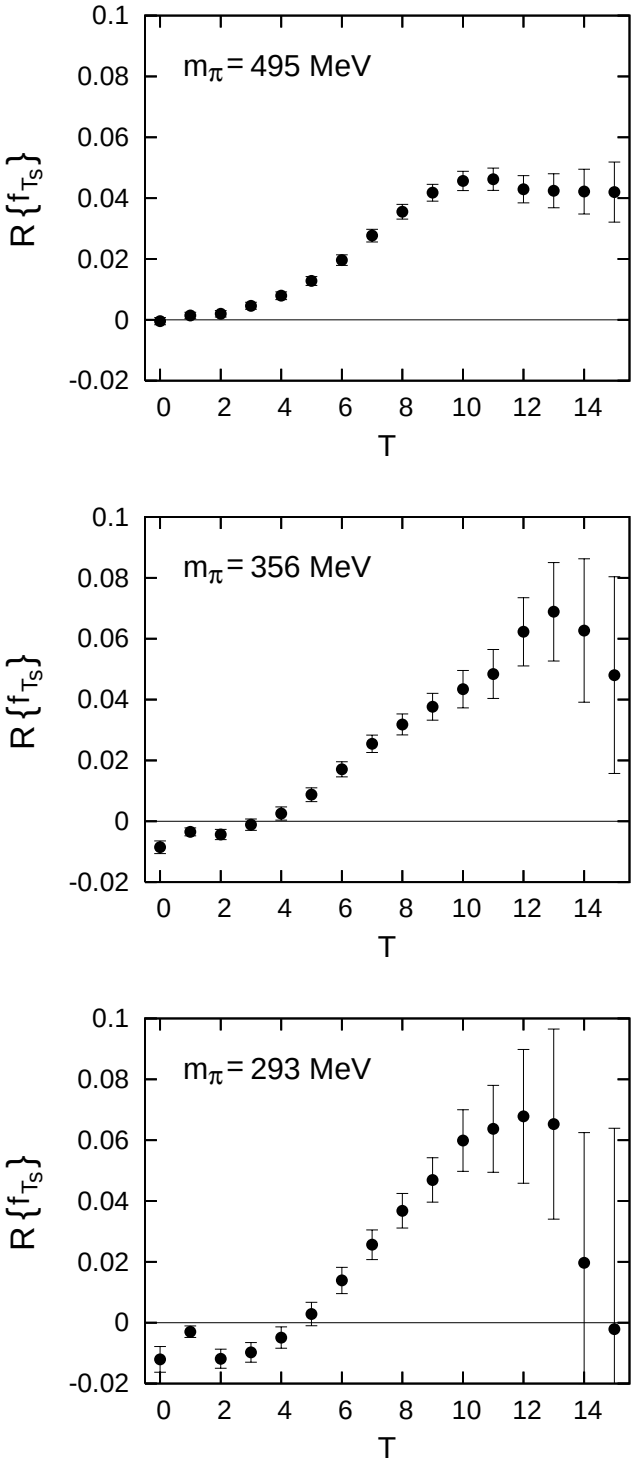

Figure 3: Correlator ratio $R\{f_{T_s}\}$, cf. (7), averaged over insertion time τ as described in section 2.2, as a function of sink time T, for the three pion masses considered.

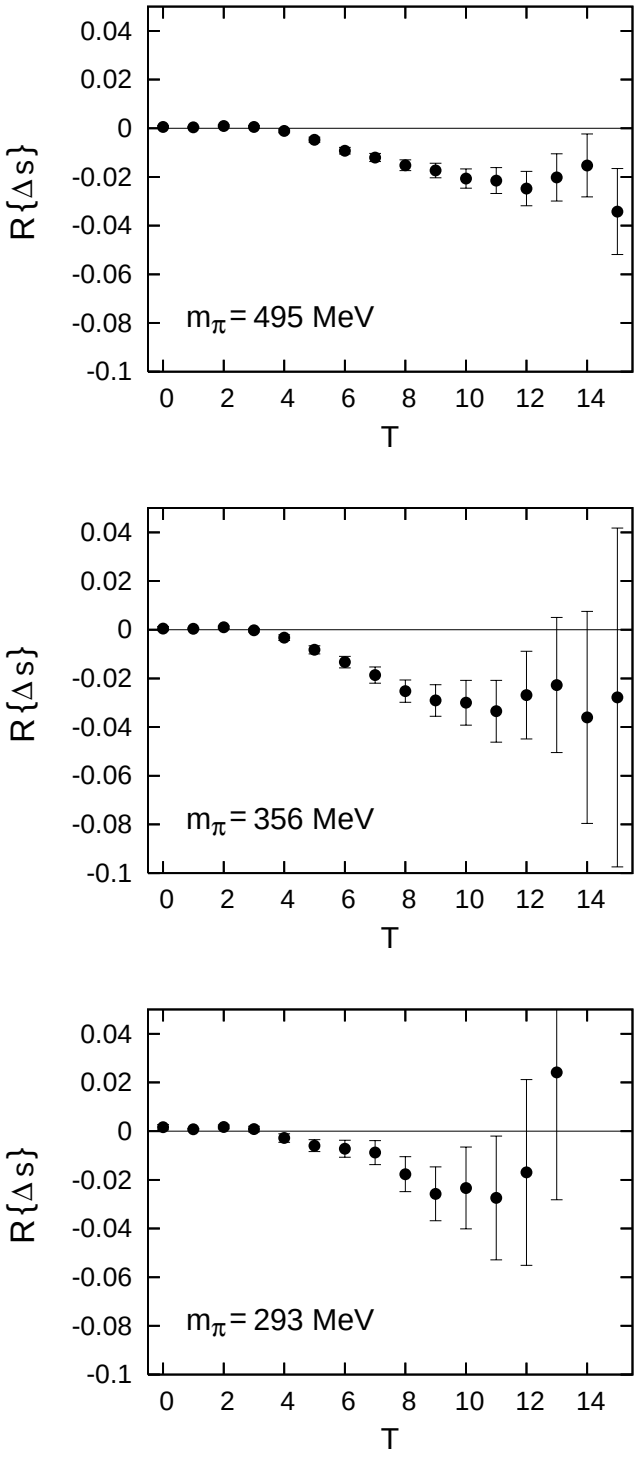

Figure 4: Correlator ratio $R\{\Delta s\}$, cf. (10), averaged over insertion time τ as described in section 2.2, as a function of sink time T, for the three pion masses considered.

m_π	$R\{f_{T_s}\}\|_{T=10}$	$R\{f_{T_s}\}\|_{T=10,\ldots,12}$
293 MeV	0.060(10)	0.064(14)
356 MeV	0.043(6)	0.051(8)
495 MeV	0.046(3)	0.045(4)

Table 3: Correlator ratio $R\{f_{T_s}\}$ at sink time $T = 10$, and averaged over $T = 10, \ldots, 12$. In the latter case, the error estimate is obtained by the jackknife method, i.e., the correlations between values of $R\{f_{T_s}\}$ at neighboring sink times are taken into account.

4 Renormalization

To establish a connection with phenomenology, quantities measured on the lattice need to be related to their counterparts in a standard renormalization scheme such as the $\overline{MS}$ scheme at a scale of 2 GeV. An advantage of the domain wall fermion discretization, used in the present treatment to represent the strange quark fields entering the quark bilinear operator insertions in the matrix elements (1) and (2), lies in its good chiral symmetry properties, which lead to a mild renormalization behavior. As a result, even though not all elements necessary for a complete renormalization of the quantities considered are available (e.g., matrix elements of gluonic operators in the nucleon, with which the flavor singlet parts of the strange quark bilinears may mix), it is possible to estimate the associated uncertainties in the renormalization, indicating that these do not dominate over the statistical uncertainties of the calculation.

4.1 Scalar matrix element

Consider first the renormalization of f_{T_s}, specifically, the proposition that the combination $m_s\langle N|\bar{s}s|N\rangle$ can be treated as independent of the renormalization scheme and scale,

$$m_s\langle N|\bar{s}s|N\rangle\big|_{\rm renorm} \stackrel{?}{=} m_s\langle N|\bar{s}s|N\rangle\big|_{\rm bare} \ . \tag{11}$$

As has been emphasized previously in [14], this behavior is contingent upon chiral symmetry being maintained in the lattice evaluation of the bare quantities. In general, the strange scalar operator $\bar{s}s$ can mix both with light quark and gluonic operators; decomposing it into flavor singlet and octet components,

$$\bar{s}s = \frac{1}{3}\left[\bar{q}q - \sqrt{3}\bar{q}\lambda_8 q\right] \tag{12}$$

(where $q \in \{u, d, s\}$), the flavor singlet part can mix with the relevant gluonic operator,

$$(\bar{q}q)^{\rm renorm} = Z_S^{00}(\bar{q}q)^{\rm bare} + Z_S^{0G}(F^2)^{\rm bare} \tag{13}$$

and also the renormalization constant Z_S^{88} of the octet part,

$$(\bar{q}\lambda_8 q)^{\rm renorm} = Z_S^{88}(\bar{q}\lambda_8 q)^{\rm bare} \tag{14}$$

in general is not identical to Z_S^{00}. However, these mixing effects would have to proceed [14] via diagrams in which the $\bar{q}q$ insertion occurs within a disconnected quark loop; furthermore, since $\bar{q}q = \bar{q}_L q_R + \bar{q}_R q_L$, a chirality flip would have to take place within that loop. Gluon vertices coupling to the loop cannot effect such a chirality flip. Thus, if all explicit chiral symmetry breaking effects are excluded, both in the dynamics as well as by adopting a mass-independent renormalization scheme, the gluonic admixture in (13) is avoided. By extension [14], also no mixing of $\bar{s}s$ with $\bar{u}u + \bar{d}d$ can take place, i.e., the renormalization factors of the flavor singlet and octet parts in (12) are equal under the assumption of strict chiral symmetry. Then, $\bar{s}s$ renormalizes in a purely multiplicative manner.

Complementarily, also the strange quark mass m_s only renormalizes multiplicatively, $m_s^{\rm renorm} = Z_m m_s^{\rm bare}$, when chiral symmetry is maintained. For generic non-chiral lattice fermion discretizations, the renormalized strange quark mass $m_s^{\rm renorm}$ acquires strong additive contributions supplementing the aforementioned multiplicative renormalization, invalidating the behavior (11). This is again avoided when chiral symmetry is respected. Indeed, when renormalization is purely multiplicative, in view of the Feynman-Hellmann theorem,

$$m_s\langle N|\bar{s}s|N\rangle = m_s\frac{\partial m_N}{\partial m_s} \ , \tag{15}$$

factors Z_m acquired by the strange quark mass under renormalization cancel on the right-hand side of (15), implying that also the left-hand side is invariant.

Chiral symmetry of the lattice fermion discretization is therefore instrumental in establishing a simple renormalization behavior of f_{T_s}, and, indeed, is realized to a good approximation in the present treatment due to the use of domain wall fermions in the coupling to the operator $\bar{s}s$. Whereas exact chiral symmetry would only be achieved using an infinite fifth dimension in the domain wall construction, in practice, the extent of this dimension has been chosen sufficiently large as to render the residual mass m_{res} quantifying the violation of chiral symmetry an order of magnitude smaller than the light quark mass in all ensembles considered [31]. One must, however, be careful in assessing the significance of this smallness, since, on the other hand, the light quark and gluonic operators with which $\bar{s}s$ mixes may have nucleon matrix elements much larger than $\langle N|\bar{s}s|N\rangle$; for $\langle N|\bar{u}u + \bar{d}d|N\rangle$, this is certainly the case. This can potentially offset the suppression of m_{res}. One may speculate that mixing with the operator $\bar{u}u + \bar{d}d$ constitutes the strongest effect, since the light quark fields are special in that they form the valence component of the nucleon, which has no counterpart in the vacuum expectation value that is subtracted off throughout, cf. (1). On the other hand, the presence of the valence quarks also strongly distorts the gluon field in the nucleon. No estimate of the gluonic admixture to $\bar{s}s$ is available, but the light quark admixture under

renormalization will be argued below to constitute an effect of the order of 1%. In view of the statistical uncertainties associated with the present determination of f_{T_s}, which amount to about 20%, a putative gluonic mixing effect would have to be an order of magnitude larger than the light quark mixing effect in order to appreciably influence the final result for f_{T_s}. This seems a rather implausible scenario. For this reason, the strong constraint on mixing with light quarks derived below will be taken as indication that violations of (11) are negligible at the present level of statistical accuracy of f_{T_s}.

Concentrating thus on the effect stemming from the mixing with the operator $\bar{u}u+\bar{d}d$, an estimate of the possible residual violation of (11) can be obtained from the Feynman-Hellmann theorem as follows [14]. The residual breaking of chiral symmetry can be parametrized to leading order via the additive mass renormalization $m_{res,q}$, which in general depends on the flavor q for which one is considering the domain wall Dirac operator,

$$m_q^{\rm renorm} = Z_m(m_q^{\rm bare} + m_{res,q}) \ . \tag{16}$$

Using (15), one has

$$\begin{aligned} m_s\langle N|\bar{s}s|N\rangle|_{\rm bare} &= m_s^{\rm bare}\sum_q \frac{\partial m_N}{\partial m_q^{\rm renorm}}\frac{\partial m_q^{\rm renorm}}{\partial m_s^{\rm bare}} \qquad (17)\\ &\approx m_s\langle N|\bar{s}s|N\rangle|_{\rm renorm} + m_s^{\rm renorm}\frac{\partial m_{res,l}}{\partial m_s^{\rm bare}}\langle N|\bar{u}u+\bar{d}d|N\rangle^{\rm renorm} \end{aligned}$$

where $m_{res,l}$ denotes the light quark flavor residual mass, and where only the dominant correction has been kept in the second line by using $m_s^{\rm bare} \gg m_{res,s}$ and $\langle N|\bar{u}u+\bar{d}d|N\rangle \gg \langle N|\bar{s}s|N\rangle$. No direct data for the factor $\partial m_{res,l}/\partial m_s^{\rm bare}$ are available, but a rough order of magnitude estimate can be constructed from related data on the residual mass obtained within the LHPC program and in the present work. This estimate is discussed in the Appendix, with the result

$$\left.\frac{\partial m_{res,l}}{\partial m_s^{\rm bare}}\right|_{m_s=0.081,m_l=0.0081} \approx -0.00035 \tag{18}$$

cf. (42), at the lowest light quark mass considered in the numerical calculations in this work. In turn, an upper bound for the light quark scalar matrix element $\langle N|\bar{u}u + \bar{d}d|N\rangle^{\rm renorm}$ is given by its magnitude at the physical point; combining a typical phenomenological value for the nucleon sigma term, $m_l\langle N|\bar{u}u + \bar{d}d|N\rangle \approx 60\,{\rm MeV}$, cf., e.g., [34] for a recent discussion, with the physical light quark mass [28], $m_l \approx 3.5\,{\rm MeV}$, yields $\langle N|\bar{u}u + \bar{d}d|N\rangle \approx 17$. Supplementing this with the value of the strange quark mass [28], $m_s = 95\,{\rm MeV}$ (all aforementioned quark masses being quoted in the $\overline{MS}$ scheme at 2 GeV), yields

$$\delta(m_s\langle N|\bar{s}s|N\rangle) \approx -0.6\,{\rm MeV} \tag{19}$$

for the correction term in the second line of (17). This would amount to a 1% upward shift of the bare result for f_{T_s} as one translates the quantity to the $\overline{MS}$ scheme at 2 GeV.

Compared to the statistical uncertainties of the present calculation, a correction of this magnitude is negligible, and in the following, (11) will therefore be taken to hold for the present calculation within its uncertainties[2].

It should again be noted that the mixing with gluonic operators has not been quantified in the above considerations. Whereas the weakness of the mixing with light quark operators (which, after all, is mediated by the coupling to the gluonic fields) makes it seem improbable that mixing with gluonic operators themselves is significant compared to other uncertainties of the calculation, explicit corroboration of this expectation would be desirable.

4.2 Axial vector matrix element

Turning to the axial vector matrix element, chiral symmetry again provides important constraints, although it cannot completely exclude mixing effects, due to its anomalous $U_A(1)$ breaking. The domain wall fermion discretization admits a five-dimensional partially conserved axial vector current $\mathcal{A}_\mu^a$ obeying a Ward-Takahashi identity of the form [35, 36]

$$\Delta_\mu \mathcal{A}_\mu^a = 2mJ_5^a + 2J_{5q}^a \tag{20}$$

The first term on the right-hand side represents the explicit breaking of chiral symmetry by the quark masses, whereas the second term in the flavor-octet case encodes the residual chiral symmetry breaking present for a fifth dimension of finite extent [36], $J_{5q}^a \approx m_{res} J_5^a$. Thus, up to these chiral symmetry breaking effects, which will be revisited further below, the flavor octet part of the current $\mathcal{A}_\mu^a$ is conserved and undergoes no renormalization. On the other hand, in the flavor singlet case, the second term on the right-hand side of (20) in addition encodes the coupling to the gluonic topological density which leads to the anomalous $U_A(1)$ breaking of chiral symmetry. This opens the possibility of operator mixing under renormalization in the flavor singlet component. With respect to direct gluonic admixtures, the axial case differs somewhat from the scalar case discussed further above. The continuum axial vector current $\mathcal{A}_\mu^{(\mathrm{cont})}$ receives no direct gluonic admixtures [37], since the relevant gluonic operator would be the operator K_μ which, upon taking the divergence, yields the gluonic topological density, $\partial_\mu K_\mu = g^2 \widetilde{F} F$. However, K_μ itself is not gauge invariant, and therefore the gauge invariant operator $\mathcal{A}_\mu^{(\mathrm{cont})}$ receives no admixtures from K_μ. While it is not clear to what extent this argument is modified at finite lattice spacing, the fact that direct gluonic admixtures to the flavor-singlet axial vector current must vanish in the continuum limit suggests that any such modifications would be small compared to the mixing of the strange quark axial current with the light quark axial currents. Concentrating thus on

[2]Note that the consideration of the factor $\partial m_{res,l}/\partial m_s^{\mathrm{bare}}$ given in the Appendix relies on a number of assumptions and should be viewed as no more than a rough estimate of what is most likely an upper bound on the magnitude of this correction factor. In view of this, applying the correction (19) to the numerical data does not seem warranted.

the latter, one can obtain a corresponding estimate of operator mixing effects as follows. Decomposing

$$\bar{s}\gamma_\mu\gamma_5 s = \frac{1}{3}\left[\bar{q}\gamma_\mu\gamma_5 q - \sqrt{3}\bar{q}\gamma_\mu\gamma_5\lambda_8 q\right] \tag{21}$$

(where $q \in \{u, d, s\}$), and allowing for different renormalization constants for the singlet and octet parts,

$$\begin{aligned}(\bar{s}\gamma_\mu\gamma_5 s)^{\text{renorm}} &= \frac{1}{3}Z_A^{00}\bar{q}\gamma_\mu\gamma_5 q - \frac{\sqrt{3}}{3}Z_A^{88}\bar{q}\gamma_\mu\gamma_5\lambda_8 q &(22)\\ &= Z_A^{88}\bar{s}\gamma_\mu\gamma_5 s + \frac{1}{3}\frac{Z_A^{00}-Z_A^{88}}{Z_A^{88}}Z_A^{88}\bar{q}\gamma_\mu\gamma_5 q &(23)\end{aligned}$$

The relative strength of mixing $(Z_A^{00} - Z_A^{88})/Z_A^{88}$ is not available for the specific lattice scheme used in the present work, but has been estimated for the case of clover fermions [11, 38]. To the extent that this encodes the effect of the axial anomaly as opposed to specific lattice discretization effects, it can be taken as indicative of the strength of mixing also in other lattice schemes such as the one used in the present investigation. Inasfar as it is influenced by the lattice scheme, it presumably can be taken to represent an upper bound for the strength of mixing in schemes which better respect chiral symmetry such as the one used here (assuming there are no accidental cancellations). Quantitatively, for the conversion into the $\overline{MS}$ scheme at the scale $\mu = 2\,\text{GeV}$, one obtains in the two-flavor clover fermion case [11]

$$\frac{Z_A^{00} - Z_A^{88}}{Z_A^{88}} = \frac{0.0082}{0.765} = 0.011 \tag{24}$$

Correcting by a factor 3/2 to translate to the three-flavor case considered here, and supplementing with $Z_A^{88} \approx 1.1$, as obtained below, as well as $\Delta(u + d) \approx 0.42$ (at the physical pion mass, cf. [33]), the uncertainty from mixing with light quarks, i.e., the second term in (23) is estimated to amount to

$$\delta(\Delta s) \approx 0.0025 \tag{25}$$

directly at the physical pion mass. Due to the indirect nature of this estimate, the shift (25) will not be applied to the (chirally extrapolated) central value for Δs obtained in this work, but will be treated as a systematic uncertainty.

It should be remarked that the considerations for the clover case [11] referred to above pertain to lattices with a substantially finer spacing than used here (0.073 fm vs. 0.124 fm). However, adjusting for this is expected to modify (25) merely by a few percent and thus is negligible in the present context. This can be inferred from the magnitude of the $O(a)$ improvement corrections to the renormalization constants quoted in [11]; note also that the present HYP-smeared mixed action scheme, which is fully $O(a)$-improved, suffers only from very benign finite lattice spacing effects, as evidenced,

e.g., by the congruence between nucleon mass measurements in this same scheme and corresponding MILC determinations on much finer, $a = 0.06\,\mathrm{fm}$ lattices [32].

Turning to the renormalization constant Z_A^{88}, the axial vector quark bilinear used in practice in evaluating Δs is the local $\bar{s}(x)\gamma_\mu\gamma_5 s(x)$ as opposed to the corresponding flavor component of the partially conserved $\mathcal{A}_\mu$ of eq. (20). To renormalize this local operator, the standard scheme [36] can be applied, with the modification that, in the present case, it is not the pion current but the η current which is relevant: Calculating the (connected parts of the) two-point functions of both the conserved and the local current,

$$\begin{aligned} C(t+1/2) &= \sum_x \langle \mathcal{A}_0^8(x,t)\ \eta(0,0)\rangle|_{\mathrm{conn}} \\ L(t) &= \sum_x \langle \bar{q}\gamma_0\gamma_5(\lambda_8/2)q\ \eta(0,0)\rangle|_{\mathrm{conn}}\ , \end{aligned} \tag{26}$$

$Z_A^{88}/Z_{\mathcal{A}}^{88}$ can be extracted from an appropriate ratio which takes into account the temporal offset between the two currents,

$$\frac{1}{2}\left(\frac{C(t+1/2)+C(t-1/2)}{2L(t)} + \frac{2C(t+1/2)}{L(t)+L(t+1)}\right) \overset{t/a\gg 1}{\longrightarrow} \frac{Z_A^{88}}{Z_{\mathcal{A}}^{88}} \tag{27}$$

Note that the full correlators $\langle \bar{q}\gamma_0\gamma_5(\lambda_8/2)q\ \eta(0,0)\rangle$ and $\langle \mathcal{A}_0^8(x,t)\ \eta(0,0)\rangle$ acquire disconnected contributions for unequal strange and light quark masses; however, for the specific purpose of extracting $Z_A^{88}/Z_{\mathcal{A}}^{88}$, any ratio of quantities which only differ by this overall renormalization factor is suitable, including using only the connected part of the aforementioned correlator, as indicated in (26). Table 4 lists the values obtained for $Z_A^{88}/Z_{\mathcal{A}}^{88}$, which are applied to the bare lattice measurements of Δs.

m_l^{bare}	0.0081	0.0138	0.0313	0.081
$Z_A^{88}/Z_{\mathcal{A}}^{88}$	1.09	1.09	1.10	1.13

Table 4: Renormalization factor $Z_A^{88}/Z_{\mathcal{A}}^{88}$ at varying m_l^{bare}.

A systematic uncertainty is associated with this scheme of renormalizing Δs, due to residual sources of chiral symmetry breaking. One of these sources is the finite extent of the fifth dimension in the domain wall fermion construction. At finite m_{res}, the renormalization constant of the partially conserved current, $Z_{\mathcal{A}}^{88}$, can deviate from the unit value it would take if chiral symmetry were strictly observed [39]. Secondly, note that, at finite lattice spacing a, there is a certain tension between adopting a mass-independent lattice renormalization scheme and maintaining $O(a)$ improvement [40]. The renormalization constant Z_A^{88} in general contains dependences of order $O(m_q a)$, evident in the slight variation displayed in Table 4. Since the lattice data necessary to

perform the continuum limit $a \to 0$ are not available, two options remain: One option would be to extrapolate $Z_A^{88}/Z_{\mathcal{A}}^{88}$ to the chiral limit, thus obtaining a mass-independent renormalization scheme in more direct correspondence to the $\overline{MS}$ scheme, but spoiling $O(a)$ improvement. On the other hand, by retaining the leading quark mass dependence, i.e., applying the finite-m_q renormalization constants in Table 4 ensemble by ensemble, $O(a)$ improvement is maintained, at the expense of introducing a slight mass dependence into the renormalization scheme at finite a. The mass dependence, implying a breaking of chiral symmetry in addition to the one encoded in the residual mass m_{res}, is then expected to be of order $O(m_q a^2)$. Since the present investigation yielded lattice data at only a single lattice spacing a, precluding a direct estimate of the effects of finite lattice spacing, maintaining $O(a)$ improvement seems sufficiently desirable to elect the latter alternative, i.e., applying the renormalization constants in Table 4 ensemble by ensemble and thus introducing a slight mass dependence into the renormalization scheme.

A way of estimating the systematic uncertainty in the renormalization of Δs resulting from the residual breaking of chiral symmetry due to the above sources lies in the mismatch between the axial vector and the vector renormalization factors, $Z_A/Z_{\mathcal{A}}$ vs. $Z_V/Z_{\mathcal{V}}$, which would remain equal if chiral symmetry were strictly maintained [41]. In the lattice scheme used here, these factors typically differ by 3% [33][3]. An additional systematic uncertainty of this magnitude will therefore be attached to the renormalized value of Δs.

5 Chiral extrapolation

Chiral extrapolation formulae for strange quark matrix elements in the nucleon have been given in [42]. At leading order (LO), both $\langle N|\bar{s}s|N\rangle$ and Δs are constant in m_π^2. On the other hand, when one evaluates one-loop effects, including Δ-resonance degrees of freedom, one obtains next-to-next-to-leading-order (NNLO) formulae which contain too many parameters to be effectively constrained by the restricted set of lattice data at three pion masses accessed in this work. However, practicable fits can be constructed by reducing the NNLO formulae given in [42] to the chiral effective theory without Δ-resonance degrees of freedom, which is achieved by setting $g_{\Delta N} = 0$ and correspondingly also eliminating the counterterms associated with the Δ-resonance degrees of freedom. In this case, the behavior of $\langle N|\bar{s}s|N\rangle$ reduces to a linear function in the light quark mass, i.e., in m_π^2,

$$\langle N|\bar{s}s|N\rangle = S_1 + S_2 m_\pi^2 \tag{28}$$

with the two fit parameters S_1 and S_2, whereas Δs retains a chiral logarithm,

$$\Delta s = D_1 \left[1 - \frac{3g_A^2}{8\pi^2 f^2} m_\pi^2 \log(m_\pi^2/\mu^2)\right] + D_2 m_\pi^2 \tag{29}$$

[3]To be precise, [33] considered the isovector currents, i.e., determined $Z_A^{33}/Z_{\mathcal{A}}^{33}$ and $Z_V^{33}/Z_{\mathcal{V}}^{33}$.

with the two fit parameters D_1 and D_2; the dependence on the scale μ is of course absorbed by the D_2 counterterm. The pion decay constant f is normalized such that $f \sim 132\,\mathrm{MeV}$, and the physical axial coupling constant is $g_A \sim 1.26$. Corresponding chiral fits to the renormalized lattice data for $m_s\langle N|\bar{s}s|N\rangle = m_N f_{T_s}$ and Δs are shown in Fig. 5. The LO constant fits and the (reduced) NNLO fits are consistent with one another. Positing the LO constant behavior in m_π^2 leads to artificially low estimates of the uncertainties; in this case, the statistical error bars are dominated by the most accurately determined $m_\pi = 495\,\mathrm{MeV}$ data points, at which, on the other hand, the chiral extrapolation formulae are the least trustworthy. Plausible estimates of the statistical uncertainties of the extrapolated values are given by the (reduced) NNLO fits, which allow for variation of the observables with m_π^2. The estimates of f_{T_s} and Δs resulting from the (reduced) NNLO fits at the physical pion mass in the $\overline{MS}$ scheme at a scale of $2\,\mathrm{GeV}$ are (before taking into account systematic effects, which are discussed in the next section),

$$f_{T_s} = 0.057(11)\ , \tag{30}$$

where the physical nucleon mass has been used to convert the fit result from Fig. 5 back to f_{T_s}, and

$$\Delta s = -0.028(14)\ . \tag{31}$$

Note again that the quoted uncertainties at this point contain only the statistical error from the lattice measurement, propagated through the chiral extrapolation; systematic uncertainties and adjustments of the results (30) and (31) are elaborated upon in the next section.

6 Systematic corrections and uncertainties

Several sources of systematic uncertainty should be taken into account with respect to the two results (30) and (31):

Renormalization uncertainties: Uncertainties associated with renormalization were already discussed in section 4. In the case of f_{T_s}, uncertainties due to mixing with light quark operators generated by residual breaking of chiral symmetry were estimated to be of the order of 1% and will thus not be considered further here. In the case of Δs, mixing effects were less well constrained because of the anomalous breaking of chiral symmetry. The potential correction to Δs was estimated to amount to $\delta(\Delta s) \approx 0.0025$ towards less negative values, cf. (25). In addition, a 3% uncertainty was assigned to the renormalization factor Z_A^{88} due to residual sources of chiral symmetry breaking. These included finite-m_{res} effects as well as effects of adopting a not fully mass-independent lattice renormalization scheme, in order to preserve $O(a)$ improvement. Adding the uncertainty from operator mixing and the one associated with Z_A^{88} in quadrature implies an uncertainty in Δs of $+0.003/-0.001$.

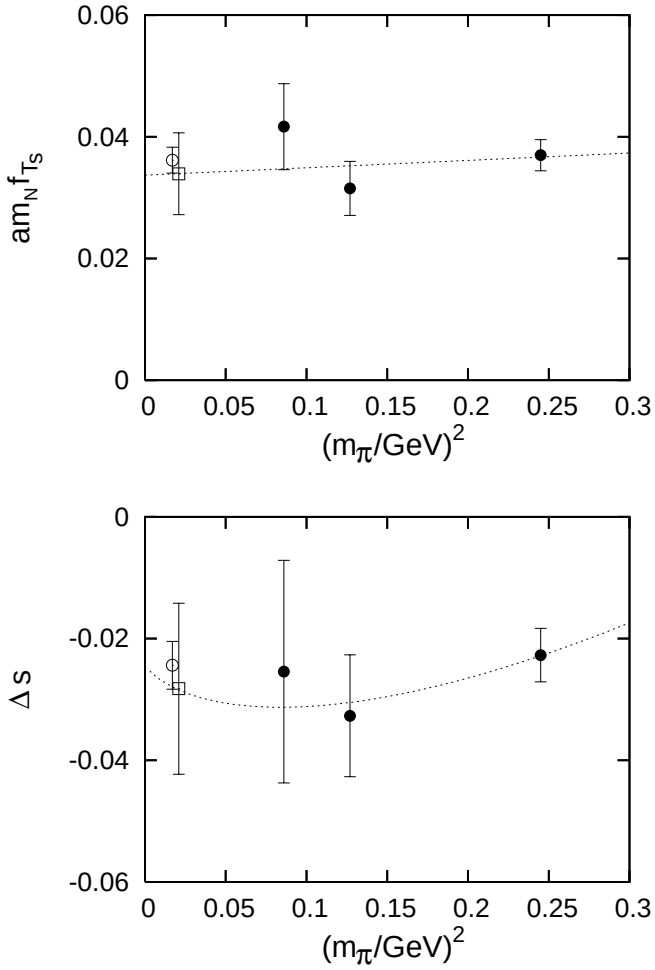

Figure 5: Pion mass dependence of the results for $m_s\langle N|\bar{s}s|N\rangle = m_N f_{T_s}$ and Δs. Filled circles represent renormalized lattice data; in the case of Δs, these are obtained by multiplying the $T = 10$ values from Table 2 by the corresponding renormalization constants from Table 4, whereas $m_N f_{T_s}$ is obtained by multiplying the $T = 10$ values from Table 3 by the corresponding nucleon masses from Table 1. Open symbols show chiral extrapolations of the lattice data to the physical pion mass, cf. main text. Open circles represent the LO (constant) chiral extrapolations, whereas open squares represent the reduced NNLO extrapolations obtained by dropping the Δ-resonance degrees of freedom, with the dashed lines showing the pion mass dependences of the central values in the latter case.

Finite lattice spacing effects: Since the present investigation only employed ensembles at a single lattice spacing, $a = 0.124\,\mathrm{fm}$, no direct assessment of the a-dependence of the results was possible. This motivated the insistence on a fully $O(a)$-improved calculational scheme, in order to minimize the influence of the finite lattice spacing from the outset (and, in the process, part of the lattice spacing dependence was already subsumed under the uncertainty in renormalization, as noted above). In the case of f_{T_s}, which is related via the Feynman-Hellmann theorem to the nucleon mass, an estimate of the uncertainty due to discretization effects can be inferred from the a-dependence of the nucleon mass. As shown in [32], already at $a = 0.124\,\mathrm{fm}$, the nucleon mass in the present HYP-smeared mixed action scheme coincides with the MILC $a = 0.06\,\mathrm{fm}$ results. Given that the MILC results themselves still change by about 10% going from $a = 0.124\,\mathrm{fm}$ to $a = 0.06\,\mathrm{fm}$, the residual $O(a^2)$ effect in the latter case is expected to be around 3%. This will therefore be taken as the generic estimate of the magnitude of finite lattice spacing effects in the present calculation, both for f_{T_s} and Δs.

Uncertainty due to truncation of the chiral perturbation series: Taking the deviation between the LO and the (reduced) NNLO fits at the physical pion mass, cf. Fig. 5, as a measure of the uncertainty due to truncation of the chiral perturbation series, a 6% uncertainty is attached to the value of f_{T_s} and a 14% uncertainty to Δs.

Effects of inadequate lattice dimensions: Both the spatial extent of the lattice and the temporal separations between nucleon source, sink and operator insertion are limited. Consequently, results are influenced both by interactions with periodic copies of the lattice as well as excited state admixtures. Neither of the corresponding uncertainties were directly quantifiable within the present calculation. On the one hand, ensembles with only a single lattice extent were employed; on the other hand, no systematic excited state effects could be gleaned from the sink position dependence of the lattice data at the present level of statistical accuracy, as discussed in section 3. An indication of the possible magnitude of such effects can be inferred from lattice calculations of the nucleon axial charge g_A, the isovector light quark analogue of Δs, which represents a well-studied benchmark quantity. Calculations of g_A within the present lattice scheme [33] and others [43, 44] exhibit a deviation from the phenomenological expectation of up to 10%, with the cause of this deviation attributed to either excited state contaminations or finite lattice size effects. This will therefore be taken as an estimate of the systematic uncertainty due to such effects also in the present calculation.

Adjustment of the strange quark mass: The strange quark mass $am_s^{asq} = 0.05$ in the gauge ensembles used in the present calculation lies appreciably above the physical strange quark mass, which a posteriori was determined to be $am_s^{asq,phys} = 0.036$ [16]. For the case of the strange scalar matrix element, a corresponding correction factor was estimated in [16], namely,

$$\frac{\partial}{\partial m_s^{asq}} \frac{\partial m_N}{\partial m_s^{asq}} = -2.2 \cdot 0.31\,\mathrm{fm} = -0.68\,\mathrm{fm} \tag{32}$$

Multiplying this by the shift in m_s^{asq}, $\delta m_s^{asq} = (0.036 - 0.05)/a$, yields, in view of the Feynman-Hellmann theorem, an enhancement of the strange scalar matrix element by

$$\delta(\langle N|\bar{s}s|N\rangle)^{asq} = \delta m_s^{asq} \frac{\partial}{\partial m_s^{asq}} \frac{\partial m_N}{\partial m_s^{asq}} = 0.077 \tag{33}$$

To translate this to the present scheme, one needs to rescale the strange quark mass, $m_s^{asq} = (m^{asq}/m^{DWF}) m_s^{DWF}$. The rescaling factor m^{asq}/m^{DWF} varies only weakly between $am_s^{asq} = 0.05$ and $am_s^{asq} = 0.02$, namely, from 0.617 in the former case to 0.639 in the latter, cf. Table 1. Interpolating linearly, the most appropriate value for the present consideration is the one halfway between $am_s^{asq} = 0.05$ and $am_s^{asq} = 0.036$, i.e., $m^{asq}/m^{DWF} = 0.622$. Since (33) has two powers of m_s^{asq} in the denominator and one in the numerator, altogether, translated to the present scheme,

$$\delta(\langle N|\bar{s}s|N\rangle)^{DWF} = \frac{m^{asq}}{m^{DWF}} \delta(\langle N|\bar{s}s|N\rangle)^{asq} = 0.048 \tag{34}$$

To obtain a measure of the relative change in $\langle N|\bar{s}s|N\rangle$ implied by this, note that the result (30), multiplied by $m_N/m_s^{DWF} = 7.3$, yields $\langle N|\bar{s}s|N\rangle^{DWF}_{am_s^{DWF}=0.081} = 0.42$, and therefore the adjustment (34) corresponds to an enhancement of $\langle N|\bar{s}s|N\rangle$ by a factor 1.115 as one shifts the strange quark mass to its physical value.

On the other hand, f_{T_s} itself acquires an additional factor $m_s^{DWF,phys}/m_s^{DWF} \approx m_s^{asq,phys}/m_s^{asq} = 0.72$ as one shifts the strange quark mass to the physical point, implying that f_{T_s} is reduced by a factor $0.72 \cdot 1.115 = 0.80$. The reduction of m_s in fact overcompensates the enhancement of $\langle N|\bar{s}s|N\rangle$. Altogether, thus, (30) will be adjusted by a factor 0.80 to arrive at the physical value; in addition, a systematic uncertainty of 3% will be associated with that adjustment in view of a 15% uncertainty in (32), cf. [16], as well as the variability in m^{asq}/m^{DWF}.

For the case of Δs, no similarly detailed consideration is available. However, it seems plausible that the leading effect of a lowering of the strange quark mass is an overall enhancement of the strange quark density, with the detailed dynamics governing any given strange quark unaffected to a first approximation. In this case, one would expect the enhancement factor 1.115 to equally apply to the axial matrix element Δs. In view of the rough nature of this argument, a systematic uncertainty of 12% will be associated with this enhancement, thus covering the range of no enhancement of Δs up to twice the enhancement seen in the case of the scalar matrix element.

Summarizing the diverse uncertainties and adjustments discussed above, the final estimates for the physical values of f_{T_s} and Δs are as follows:

$$f_{T_s} = 0.046(9)(1)(3)(5)(1) \tag{35}$$

where the uncertainties are, in the order written, statistical, due to finite lattice spacing, due to truncation of the chiral perturbation series, due to inadequate lattice dimensions,

and due to the adjustment of the strange quark mass to the physical value. In turn,

$$\Delta s = -0.031(16)(^{+3}_{-1})(1)(4)(3)(4) \tag{36}$$

where the uncertainties are, in the order written, statistical, due to renormalization, due to finite lattice spacing, due to truncation of the chiral perturbation series, due to inadequate lattice dimensions, and due to the adjustment of the strange quark mass to the physical value. To quote a succint final result, if one combines all the systematic uncertainties discussed in this section together with the statistical uncertainty in quadrature,

$$f_{T_s} = 0.046(11) \tag{37}$$

$$\Delta s = -0.031(17) \tag{38}$$

7 Conclusions

This investigation focused on two of the most basic signatures of strange quark degrees of freedom in the nucleon, namely, the strange quark contribution to the nucleon mass, characterized by f_{T_s}, and the portion of the nucleon spin contained in strange quark spin, Δs. A high amount of averaging not only of the disconnected strange quark loop, but also of the nucleon two-point function led to clear signals for both f_{T_s} and Δs especially at the heaviest pion mass, $m_\pi = 495\,\mathrm{MeV}$, with the signals deteriorating, but not disappearing, as the pion mass is lowered to $m_\pi = 356\,\mathrm{MeV}$ and $m_\pi = 293\,\mathrm{MeV}$. Combining all the lattice data, the signals survive chiral extrapolation to the physical pion mass. Systematic uncertainties remain under adequate control; the only source of systematic uncertainty which was not quantified is gluonic operator admixtures to f_{T_s} under renormalization. However, as discussed in section 4.1, a scenario in which these admixtures rise to the level at which they begin to appreciably influence the conclusions reached regarding f_{T_s} seems highly implausible. The gluonic admixtures would have to be an order of magnitude larger than the related light quark admixtures, which were constrained to the 1% level. Nevertheless, a more quantitative corroboration of this argument would be desirable. All other systematic uncertainties were quantified, cf. section 6, and, while some of them are still sizeable, none rise to the level of the statistical uncertainties. With respect to controlling systematic uncertainties, the use of a (to a very good approximation) chirally symmetric discretization of the strange quark fields in the matrix elements (1),(2) proved very advantageous, since it provides for benign renormalization properties, including the almost complete suppression of light quark admixtures to f_{T_s} alluded to above. This stands in contrast to, e.g., the case of Wilson fermions, in which the evaluation of f_{T_s} is considerably complicated by the presence of strong additive mass renormalizations [12, 24].

The magnitudes obtained for both f_{T_s} and Δs appear natural. Neither quantity is abnormally enhanced; strange quarks contribute about 4.5% of the nucleon mass, and

the magnitude of the strange quark spin, which is polarized opposite to the nucleon spin, amounts to about 3% of the latter. The conditions provided by nucleon structure for dark matter detection via coupling of the Higgs field specifically to the strange quark component thus do not appear to be as favorable as assumed in the most optimistic scenaria. There is also no indication from the result for Δs that an unnaturally large contribution to the spin of the nucleon is hidden in the small-x strange quark sector that has hitherto eluded experimental study. The strange quark spin does indeed appear to be polarized slightly in the direction opposite to the nucleon spin, as also indicated by the preponderance of phenomenological studies. However, the magnitude of Δs found in the present calculation is smaller than the magnitudes extracted in the analyses [5, 9] which assume a substantial enhancement of the strange quark helicity distribution at small momentum fraction x.

Acknowledgments

Fruitful exchanges with W. Freeman, H. Grießhammer, P. Hägler, K. Orginos, S. Pate and D. Toussaint are gratefully acknowledged. The computations required for this investigation were carried out at the Encanto computing facility operated by NMCAC, using the Chroma software suite [45] and gauge ensembles provided by the MILC Collaboration. This work was supported by the U.S. DOE under grant DE-FG02-96ER40965.

Appendix: Estimate of $\partial m_{res,l}/\partial m_s^{\mathbf{bare}}$

The quantity $\partial m_{res,l}/\partial m_s^{\mathrm{bare}}$ enters the estimate of operator mixing effects in f_{T_s}, cf. section 4.1. No direct data for this quantity are available, but an order of magnitude estimate can be constructed from related data on the residual mass obtained within the LHPC program and in the present work, summarized in Table 5. It should be noted

m_l^{bare}	0.0081	0.0313	0.081
$10^3 \cdot m_{res,l}$	1.6	1.2	0.7
$10^4 \cdot m_{res,s}$	9.0	8.1	7.1

Table 5: Residual masses $m_{res,l}$ and $m_{res,s}$ at varying m_l^{bare}.

that all these results were obtained at a constant lattice spacing a. Fitting parabolae to the data in Table 5 yields the following derivatives at the $SU(3)$-flavor symmetric point $m_s = m_l = 0.081$ and at the lightest m_l considered in this work, $m_l = 0.0081$:

$$\left.\frac{\partial m_{res,l}}{\partial m_l^{\mathrm{bare}}}\right|_{m_s=m_l=0.081} = -0.005 \qquad \left.\frac{\partial m_{res,l}}{\partial m_l^{\mathrm{bare}}}\right|_{m_s=0.081,m_l=0.0081} = -0.020 \qquad (39)$$

$$\left.\frac{\partial m_{res,s}}{\partial m_l^{\rm bare}}\right|_{m_s=m_l=0.081} = -0.0007 \qquad \left.\frac{\partial m_{res,s}}{\partial m_l^{\rm bare}}\right|_{m_s=0.081,m_l=0.0081} = -0.0045 \quad (40)$$

The simplest estimate for $\partial m_{res,l}/\partial m_s^{\rm bare}$ from this can be obtained by noting that, at the $SU(3)$-flavor symmetric point,

$$\left.\frac{\partial m_{res,l}}{\partial m_s^{\rm bare}}\right|_{m_s=m_l=0.081} = \frac{1}{2}\left.\frac{\partial m_{res,s}}{\partial m_l^{\rm bare}}\right|_{m_s=m_l=0.081} = -0.00035 \quad (41)$$

(where the factor 1/2 stems from the fact that $\partial/\partial m_l = \partial/\partial m_u + \partial/\partial m_d$). Assuming that the derivative of $m_{res,l}$ in the m_s-direction varies only weakly as one changes m_l, one arrives at the estimate that also

$$\left.\frac{\partial m_{res,l}}{\partial m_s^{\rm bare}}\right|_{m_s=0.081,m_l=0.0081} \approx -0.00035 \quad (42)$$

Note that this is most likely an upper bound in magnitude, since one would expect the characteristics of the gauge fields entering the Dirac operator to be dominated by the light quark degrees of freedom relative to the strange quark degrees of freedom as m_l becomes smaller.

A check on this estimate can be constructed by the following alternative chain of reasoning. First, note that the quantity $\partial m_{res,l}/\partial m_l^{\rm bare}$ contains two contributions, namely, one from the explicit variation of m_l in the Dirac operator which $m_{res,l}$ characterizes, and the other from the implicit dependence of the gauge field ensemble on m_l. To estimate $\partial m_{res,l}/\partial m_s^{\rm bare}$, one therefore needs to apply two correction factors to $\partial m_{res,l}/\partial m_l^{\rm bare}$: A factor characterizing the proportion of the variation of $m_{res,l}$ due specifically to the implicit variation of the gauge fields, and a factor characterizing the strength of that variation with m_s as opposed to m_l. The order of magnitude of these correction factors can be inferred as follows. The former factor is available at the $SU(3)$-flavor symmetric point as the ratio

$$\left.\frac{\partial m_{res,s}/\partial m_l^{\rm bare}}{\partial m_{res,l}/\partial m_l^{\rm bare}}\right|_{m_s=m_l=0.081} = 0.14\ . \quad (43)$$

For the purposes of the present argument, it will be assumed that this factor only varies mildly as $m_l^{\rm bare}$ is lowered to $m_l^{\rm bare} = 0.0081$. On the other hand, assume also that

$$\left.\frac{\partial m_{res,s}}{\partial m_s^{\rm bare}}\right|_{{\rm implicit},m_l=0.081} \approx \left.\frac{\partial m_{res,s}}{\partial m_s^{\rm bare}}\right|_{{\rm implicit},m_l=0.0081} \quad (44)$$

i.e., the implicit variation of $m_{res,s}$ via the dependence of the gauge fields on m_s changes only mildly as a function of m_l. Note that, while this assumption is analogous to the one leading to (42), it is better founded since $m_{res,s}$ itself varies less with m_l than $m_{res,l}$.

Again, one would expect the left-hand side to represent an upper bound for the right-hand side. Noting that the left-hand side is identical to one-half the quantities in the left-hand identity in (40), one thus has

$$0.08 = \frac{-0.0007/2}{-0.0045} = \frac{\partial m_{res,s}/\partial m_s^{\rm bare}|_{{\rm implicit},m_l=0.081}}{\partial m_{res,s}/\partial m_l^{\rm bare}|_{m_l=0.0081}} \tag{45}$$

$$\approx \left.\frac{\partial m_{res,s}/\partial m_s^{\rm bare}|_{\rm implicit}}{\partial m_{res,s}/\partial m_l^{\rm bare}}\right|_{m_l=0.0081} \tag{46}$$

$$\approx \left.\frac{\partial m_{res,l}/\partial m_s^{\rm bare}}{\partial m_{res,l}/\partial m_l^{\rm bare}|_{\rm implicit}}\right|_{m_l=0.0081} \tag{47}$$

where in the final step it is assumed that changes in the numerator and denominator due to changing the quark mass in the Dirac operator from m_s to m_l approximately cancel[4]. This is the desired conversion factor characterizing the strength of the implicit variation of $m_{res,l}$ with m_s relative to the one with m_l. Correcting, as proposed above, $\partial m_{res,l}/\partial m_l^{\rm bare}$ by the two factors (43) and (47), one finally arrives at the alternative estimate

$$\left.\frac{\partial m_{res,l}}{\partial m_s^{\rm bare}}\right|_{m_s=0.081,m_l=0.0081} \approx 0.08 \cdot 0.14 \cdot (-0.020) = -0.0002 \ , \tag{48}$$

consistent in order of magnitude with (42), especially in view of the latter being expected to represent an overestimate.

The estimate (42) for $\partial m_{res,l}/\partial m_s^{\rm bare}$ at the lowest light quark mass considered in the numerical calculations in this work is used in section 4.1 to constrain the influence of operator mixing effects in the renormalization of f_{T_s}.

References

[1] A. Bottino, F. Donato, N. Fornengo and S. Scopel, Astropart. Phys. **18** (2002) 205.

[2] J. Ellis, K. A. Olive, Y. Santoso and V. C. Spanos, Phys. Rev. **D 71** (2005) 095007.

[3] J. Ellis, K. A. Olive and C. Savage, Phys. Rev. **D 77** (2008) 065026.

[4] G. Bertone, ed., *"Particle Dark Matter: Observations, Models and Searches"*, Cambridge University Press, 2010.

[5] A. Airapetian et al. (HERMES Collaboration), Phys. Rev. **D 75** (2007) 012007.

[6] A. Airapetian et al. (HERMES Collaboration), Phys. Lett. **B666** (2008) 446.

[4] Individually, one can estimate the denominators in (46) and (47) to differ by somewhat less than a factor of two, by comparing the right-hand identity in (40) with the right-hand identity in (39), corrected by the factor (43).

[7] M. Alekseev et al. (COMPASS Collaboration), Phys. Lett. **B680** (2009) 217.

[8] S. Pate, D. McKee and V. Papavassiliou, Phys. Rev. **C 78** (2008) 015207.

[9] M. Alekseev et al. (COMPASS Collaboration), Phys. Lett. **B660** (2008) 458.

[10] G. Bali, S. Collins and A. Schäfer, Comput. Phys. Commun. **181** (2010) 1570.

[11] G. Bali, S. Collins, M. Göckeler, R. Horsley, Y. Nakamura, A. Nobile, D. Pleiter, P. Rakow, A. Schäfer, G. Schierholz and J. Zanotti (QCDSF Collaboration), Phys. Rev. Lett. **108** (2012) 222001.

[12] G. Bali, S. Collins, M. Göckeler, R. Horsley, Y. Nakamura, A. Nobile, D. Pleiter, P. Rakow, A. Schäfer, G. Schierholz, A. Sternbeck and J. Zanotti (QCDSF Collaboration), Phys. Rev. **D 85** (2012) 054502.

[13] H. Ohki, H. Fukaya, S. Hashimoto, T. Kaneko, H. Matsufuru, J. Noaki, T. Onogi, E. Shintania and N. Yamada (JLQCD Collaboration), Phys. Rev. **D 78** (2008) 054502.

[14] K. Takeda, S. Aoki, S. Hashimoto, T. Kaneko, J. Noaki and T. Onogi (JLQCD Collaboration), Phys. Rev. **D 83** (2011) 114506.

[15] H. Ohki, K. Takeda, S. Aoki, S. Hashimoto, T. Kaneko, H. Matsufuru, J. Noaki and T. Onogi (JLQCD Collaboration), arXiv:1208.4185.

[16] D. Toussaint and W. Freeman (MILC Collaboration), Phys. Rev. Lett. **103** (2009) 122002.

[17] W. Freeman and D. Toussaint (MILC Collaboration), arXiv:1204.3866.

[18] T. Doi, M. Deka, S.-J. Dong, T. Draper, K.-F. Liu, D. Mankame, N. Mathur and T. Streuer, Phys. Rev. **D 80** (2009) 094503.

[19] M. Gong, A. Li, A. Alexandru, T. Draper and K.-F. Liu (χQCD Collaboration), PoS **(Lattice 2011)** 156.

[20] K.-F. Liu, M. Deka, T. Doi, Y. B. Yang, B. Chakraborty, Y. Chen, S. J. Dong, T. Draper, M. Gong, H. W. Lin, D. Mankame, N. Mathur and T. Streuer (χQCD Collaboration), PoS **(Lattice 2011)** 164.

[21] S. Dürr, Z. Fodor, T. Hemmert, C. Hoelbling, J. Frison, S. Katz, S. Krieg, T. Kurth, L. Lellouch, T. Lippert, A. Portelli, A. Ramos, A. Schäfer and K. Szabo, Phys. Rev. **D 85** (2012) 014509.

[22] S. Dinter, V. Drach, R. Frezzotti, G. Herdoiza, K. Jansen and G. Rossi (ETM Collaboration), JHEP **1208** (2012) 037.

[23] R. Horsley, Y. Nakamura, H. Perlt, D. Pleiter, P. Rakow, G. Schierholz, A. Schiller, H. Stüben, F. Winter and J. Zanotti (QCDSF and UKQCD Collaborations), Phys. Rev. **D 85** (2012) 034506.

[24] R. Babich, R. Brower, M. Clark, G. Fleming, J. Osborn, C. Rebbi and David Schaich, Phys. Rev. **D 85** (2012) 054510.

[25] R. Young and A. Thomas, Phys. Rev. **D 81** (2010) 014503.

[26] P. Shanahan, A. Thomas and R. Young, arXiv:1205.5365.

[27] C. Alexandrou, K. Hadjiyiannakou, G. Koutsou, A. Ó Cais and A. Strelchenko, Comput. Phys. Commun. **183** (2012) 1215.

[28] J. Beringer et al. (Particle Data Group), Phys. Rev. **D 86** (2012) 010001.

[29] J. Liu, R. D. McKeown and M. Ramsey-Musolf, Phys. Rev. **C 76** (2007) 025202.

[30] M. Engelhardt, PoS **(Lattice 2010)** 137.

[31] P. Hägler, W. Schroers, J. D. Bratt, R. G. Edwards, M. Engelhardt, G. Fleming, B. Musch, J. W. Negele, K. Orginos, A. V. Pochinsky, D. Renner and D. G. Richards (LHP Collaboration), Phys. Rev. **D 77** (2008) 094502.

[32] A. Walker-Loud, H.-W. Lin, D. G. Richards, R. G. Edwards, M. Engelhardt, G. Fleming, P. Hägler, B. Musch, M.-F. Lin, H. B. Meyer, J. W. Negele, A. V. Pochinsky, M. Procura, S. Syritsyn, C. Morningstar, K. Orginos, D. Renner and W. Schroers, Phys. Rev. **D 79** (2009) 054502.

[33] J. D. Bratt, R. G. Edwards, M. Engelhardt, P. Hägler, H.-W. Lin, M.-F. Lin, H. B. Meyer, B. Musch, J. W. Negele, K. Orginos, A. V. Pochinsky, M. Procura, D. G. Richards, W. Schroers and S. Syritsyn (LHP Collaboration), Phys. Rev. **D 82** (2010) 094502.

[34] J. M. Alarcón, J. Martin Camalich and J. A. Oller, Phys. Rev. **D 85** (2012) 051503.

[35] V. Furman and Y. Shamir, Nucl. Phys. **B439** (1995) 54.

[36] T. Blum, P. Chen, N. Christ, C. Cristian, C. Dawson, G. Fleming, A. Kaehler, X. Liao, G. Liu, C. Malureanu, R. Mawhinney, S. Ohta, G. Siegert, A. Soni, C. Sui, P. Vranas, M. Wingate, L. Wu and Y. Zhestkov, Phys. Rev. **D 69** (2004) 074502.

[37] P. Breitenlohner, D. Maison and K. Stelle, Phys. Lett. **B134** (1984) 63.

[38] A. Skouroupathis and H. Panagopoulos, Phys. Rev. **D 79** (2009) 094508.

[39] C. Allton, D. J. Antonio, Y. Aoki, T. Blum, P. A. Boyle, N. H. Christ, S. D. Cohen, M. A. Clark, C. Dawson, M. A. Donnellan, J. M. Flynn, A. Hart, T. Izubuchi, A. Jüttner, C. Jung, A. D. Kennedy, R. D. Kenway, M. Li, S. Li, M.-F. Lin, R. D. Mawhinney, C. M. Maynard, S. Ohta, B. J. Pendleton, C. T. Sachrajda, S. Sasaki, E. E. Scholz, A. Soni, R. J. Tweedie, J. Wennekers, T. Yamazaki and J. M. Zanotti (RBC and UKQCD Collaborations), Phys. Rev. **D 78** (2008) 114509.

[40] M. Lüscher, S. Sint, R. Sommer and P. Weisz, Nucl. Phys. **B478** (1996) 365.

[41] Y. Aoki, R. Arthur, T. Blum, P. A. Boyle, D. Brömmel, N. H. Christ, C. Dawson, J. M. Flynn, T. Izubuchi, X.-Y. Jin, C. Jung, C. Kelly, M. Li, A. Lichtl, M. Lightman, M.-F. Lin, R. D. Mawhinney, C. M. Maynard, S. Ohta, B. J. Pendleton, C. T. Sachrajda, E. E. Scholz, A. Soni, J. Wennekers, J. M. Zanotti and R. Zhou (RBC and UKQCD Collaborations), Phys. Rev. **D 83** (2011) 074508.

[42] J.-W. Chen and M. Savage, Phys. Rev. **D 66** (2002) 074509.

[43] T. Yamazaki, Y. Aoki, T. Blum, H.-W. Lin, M.-F. Lin, S. Ohta, S. Sasaki, R. J. Tweedie and J. M. Zanotti (RBC and UKQCD Collaborations), Phys. Rev. Lett. **100** (2008) 171602.

[44] J. R. Green, M. Engelhardt, S. Krieg, J. W. Negele, A. V. Pochinsky and S. N. Syritsyn, arXiv:1209.1687.

[45] R. G. Edwards and B. Joó (LHPC and UKQCD Collaborations), Nucl. Phys. Proc. Suppl. **140** (2005) 832.